Modeling rainy cells observed in radar echoes

O.RAAF[1] and A.E.H. ADANE[1]

[1]*Telecommunication department*, Faculty of Electronics and Computer Science
University of Science and Technology of Algiers (USTHB) ,
Po box 32 El Alia, Bab Ezzouar 16111, Algeria

oraaf@usthb.dz, tiregz@yahoo.fr

Abstract

The propagation of electromagnetic waves with very short wavelengths is affected by the presence of various moving targets in suspension in the atmosphere. In particular, for the radars which are intended for the surveillance of the air space, the presence of atmospheric echoes of sufficiently high reflectivity produces a non-negligible interference. This paper deals with the analysis of atmospheric clutter caused by the presence of precipitating clouds. Considering the reflectivity recorded in each pixel, we have calculated and represented the mean variation of the reflectivity factor. by seeing these distributions, we notice that the experimental distribution of the reflectivity radar echoes is well modeled as a log-normal distribution or a beta distribution with a coefficient of correlation upper then 0.9.

1. Introduction

The study and analysis of cloud progress has been the subject of several scientific works in recent years. To account for these phenomena, most meteorological networks are now equipped with automatic measurement systems and remote sensing tools [1]. In particular, different geostationary satellites intended to meteorological observations, orbit the Earth in the equatorial plane for about thirty years. Radars, Lidars and Sodars are other remote sensing systems used to collect meteorological data characterising the air motions and cloud formations in the atmosphere [2, 3]. RADAR acronym for RAdio, Detection And Ranging is an electronic system used to detect the presence and determine the distance to an obstacle. The antenna of radar emits strong radio waves at high frequency and receives the reflected echoes. The analysis of the reflected signal can locate the reflector, and sometimes can identify it [2]. Weather radar, used for atmospheric sounding, can detect the presence of precipitations (water drops, snow) and to estimate the rate of rain in a given area. Thus, the radar is able to observe the precipitation fields extending over more than one hundred thousand km2. It brings every moment, information on precipitation intensity, expressed in terms of reflectivity, and their spatial distribution [3, 4]. The characterization of rain fields allows finding a signature, a feature permitting their recognition, their distinctions and predicting their movements.

Fourier analysis offers a good approach to modulate the rain echoes whereas any notion of location in time (or space) disappears in Fourier space [5]. This paper deals with the modeling of atmospheric echoes with the log-normal and Beta function. The purpose of the research is to define a function that describes the evolution of the rain cluster in order to remove it in the observing aviation space

2. Data base

The National Office of Meteorology offers a rainfall observation network consisting of seven radars mainly distributed in north of Algeria. These radars are equipped with a scanning system integration, visualization and data transmission, called SANAGA. In this paper we use the radar of Setif in the mount of Maghras. It is non-coherent pulsed radar, installed at 1700m west of Setif and works in 5.6 Ghz with a peak power of 250 kW. The duration of the radar pulse is 2 microseconds and its recurrence period of 4ms with a sensitivity of - 105 dBm at the reception. The antenna is a parabolic of 3 m in diameter and with a gain equal to 30 dB.

For this study, we have collected images every fifteen minutes during the period of January 2001. These images were obtained in the PPI representation in the format 512 x 512 pixels, with a resolution of 1 km per pixel and 16 gray levels. Images animation shows that the clouds are more frequent and denser in mountainous areas while they are rare in the southern regions. As shown in Fig. 1, the radar lies at the centre of the image, the ground echoes are represented by dark blue, yellow, orange and red color. For example, the orange band appearing at the west of Setif, is identified to the Djurdjura mountains which reach at 2308 m at their highest peak, namely Lalla Khadidja. The dark blue zones lying at the south-east and north-east of the radar represent the mounts of Bibans and Babor respectively. This variability is primarily due to the geographical characteristics of the Setif region.

The animated image analysis shows that clouds are more frequent and denser than in the mountainous areas while they are rare in the southern regions. This variability is primarily due to the geographical characteristics of the Setif region. Thus, in the case of the northeast of Algeria, the relief is quite tormented because formed of mountains, hills, plains, valleys and a sea area.

To assess this variability, we conducted an analysis of the images mesh. To do this, a square area of 180 x 180 km^2 area centered on radar, has been delineated in each of the images to be processed. This surface was then divided into nine meshes of 60 x 60 km^2 each. By adopting such a partition, our goal is to characterize the atmospheric echoes according to geographical particularities of each mesh. Fig. 1 illustrates the division into nine zones of the experimental region in one of the images studied. Our study consists, first of all, in the suppression of the parasites echoes resulting from the earth's surface in particular owed to the mountain relief by using the method of template

associated with pattern recognition developed in our laboratory [5].

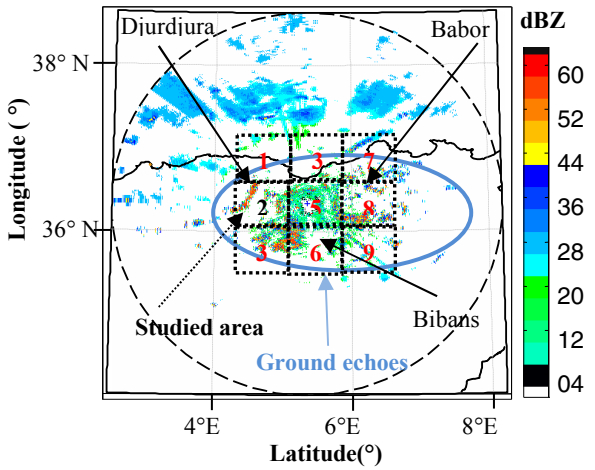

Fig. 1. Radar images collected in rainy period

Ground echoes are mostly fixed, intense and localized while rain echoes, extend over large areas which the form changes over the time with a less intense reflectivity. Various filtering techniques exist and are used to reduce the ground clutter either by implementing electronic devices or algorithms of image processing. The technique used in this paper to filter the radar images is based on the construction of templates. For this purpose, 76908 images of clear sky have first been selected by animated radar images. Then, an image of ground echoes was built by averaging all clear sky images. It is composed of pixels whose level of reflectivity is the most frequent. This image is compared, pixel by pixel, with each raw image of the database. When the pixels of the two kinds of images have the same level of reflectivity, they are replaced by zero reflectivity in the original images. Otherwise, the pixels preserve their initial reflectivity. This filter eliminates a great part of the ground clutter. However, several small ground cells remain. Indeed, a preliminary analysis of the shape of radar echoes showed that the rainy cloud surface is greater than 30 km2 while the remaining spots is much smaller. A pattern recognition algorithm based on this analysis detects all remaining ground cells and removes them. This algorithm operates by exploring the image pixel by pixel with an analysis window of 3x3 pixels. It is composed of the following steps [5]:

- This analysis window is centered on a pixel surrounded by eight nearest neighbors.
- The form of the echoes is detected by counting, for each pixel of the image, the number of neighbors whose reflectivity is not zero.
- If five nearest neighbors have zero reflectivity, the analyzed pixel is replaced by zero reflectivity. If more than three of its neighbors have a non-zero reflectivity, that pixel is kept unchanged. The pixel is then stored with its coordinates and reflectivity value.
    - The surface of each detected shape is estimated by counting the pixels that compose it. This surface is recorded if it is greater than 30 km^2, because it is considered as a rain echo. Otherwise, the cell is deleted because it is an undesirable spots.

Fig.2 represents the result of the filtering of the image of Fig.1 by pattern recognition algorithm. The filtered image shows that the rain cells are suitably restored and that all the ground echoes have been eliminated. So ground echoes could be effectively removed without altering the precipitation echoes.

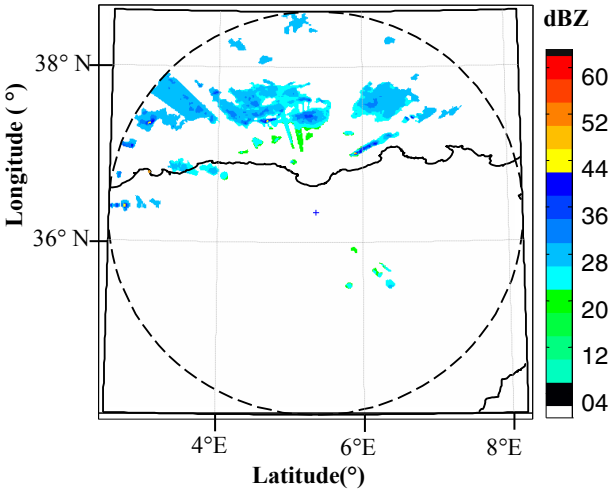

Fig. 2. Filtered Radar images

3. Statistical properties of reflectivity factor

Changes in the radar reflectivity factor (Z) over time were represented as time series. For each image, we calculated the average reflectivity factors characterizing the study area. Let Z (m, n), the reflectivity factor of pixel of coordinates (m, n). The mean (Z) of the reflectivity is defined by:

$$\overline{Z} = \frac{1}{3600} \sum_{m=1}^{N} \sum_{n=1}^{N} Z(m, n) \qquad (1)$$

As shown in Fig.3, each of the nine meshes study is then characterized by a time series describing variations of the reflectivity factor with time. Comparing the nine time series thus obtained, highlights a clear difference in rain intensity between the regions close to the Mediterranean and the southern regions. These curves also show that the value of the most important Z factor is obtained for the area that includes the chain of Djurdjura. Since this parameter is linked to precipitation rate (R) by the number of raindrops and diameter, we deduce then it rains more in the Djurdjura region. The rainfall is also important in regions encompassing the mountains of Babors and Bibans.

As shown in Fig.3 the area of study is then characterized by a time series describing the variations of the reflectivity factor over the time during two month January and February 1999.

According to the curves of Fig. 3, there is a difference in intensity between the east and the west, because that the heavy clouds come from the Mediterranean, precipitate quite frequently in the east regions. It also shows that atmospheric convection is less intense on the sea as on the ground, because the temperature is more homogeneous on the sea than on ground. To better appreciate this difference, we built the experimental frequency distributions of reflectivity factor from each of these nine time series.

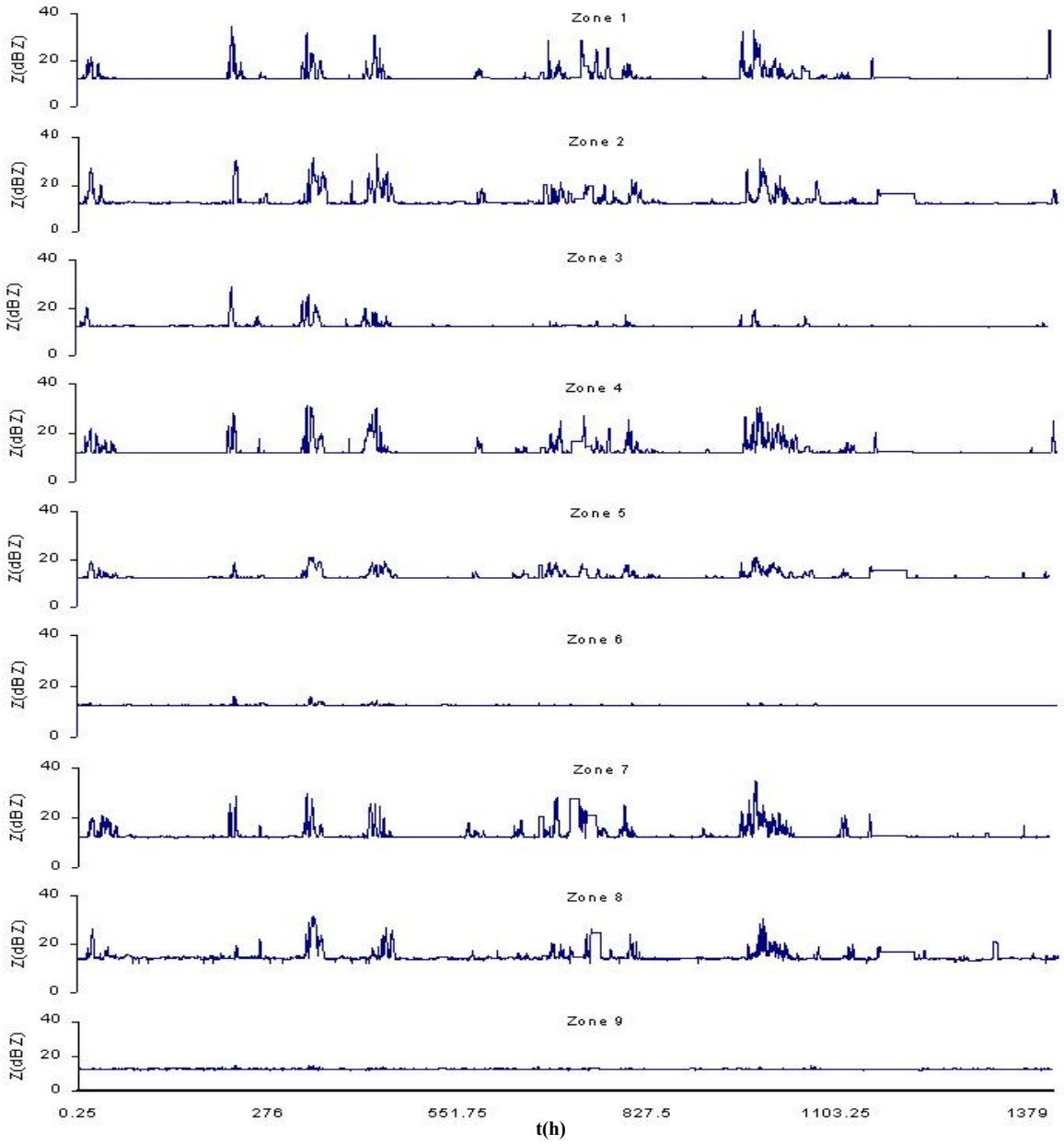

Fig. 3. Mean reflectivity variations over the time of the nine studied regions

Fig.4 gives the probability that the reflectivity factor takes one of sixteen levels of color for each of the nine studied region. These frequency distributions are all slightly asymmetrical and are well suited to a description by either a distribution lognormal or by a beta distribution. Subsequently, we chose to study area 2 because it is the rainiest area in northern Algeria as it includes the mountains of Djurdjura.

3.1. Log-normal distribution

The probability density relative to this distribution is [6]:

$$P(Z, m_y, \sigma_y) = \frac{1}{\sqrt{2\pi}\, Z\, \sigma_y} \exp\left[-\frac{1}{2}\left(\frac{\ln Z - m_y}{\sigma_y}\right)\right] \qquad (2)$$

The parameters of the log - normal distribution are respectively calculated by:

$$m_y = \ln m_Z - \frac{1}{2}\ln\left(1+\frac{\sigma_Z^2}{m_Z^2}\right) = \ln\left(\frac{m_Z}{\sqrt{1+CV_Z^2}}\right) \qquad (3)$$

$$\sigma_y^2 = \ln\left(1+\frac{\sigma_Z^2}{m_y}\right) = \ln\left(\left(1+CV_Z^2\right)\right) \qquad (4)$$

With :

$$CV_Z = \frac{\sigma_Z}{m_Z} = \sqrt{\exp(\sigma_y^2 - 1)} \qquad (5)$$

Where mz is the mean and σz is the standard deviation of *Z*.

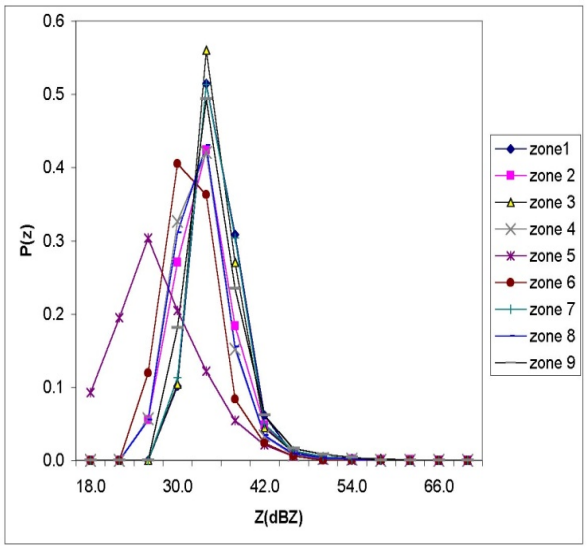

Fig. 4. Density probability function of the nine studied regions

Using the numerical values of mz and σz deducted from the time series of Fig.3, we obtain the curves shown in Fig.5. In this figure, the curves obtained experimentally, are shown in green lines. It finds that the two probability distribution types are slightly different from each other and the correlation coefficient relating the measured and calculated values is substantially 0.9. This result indicates that the reflectivity factor and then the reflectivity radar is well suited represented by a log-normal distribution, but the parameters of this distribution differs from one area to another depending on the morphology of the area.

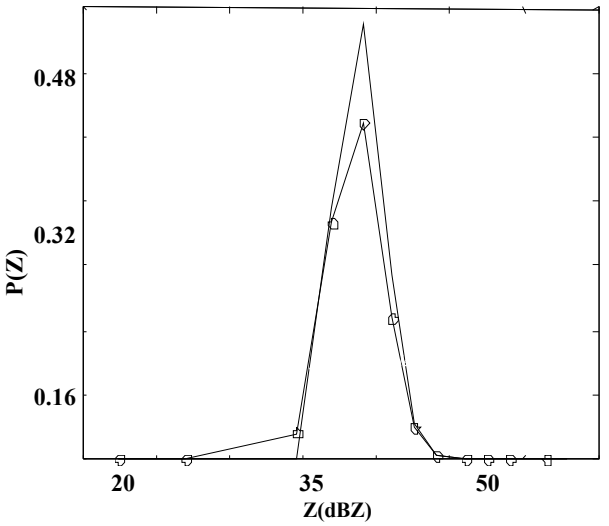

Fig. 5. Lognormal distribution associated with the log(z) for the study area ((o) experimental distribution (-) lognormal distribution).

3.2. Beta distribution

Let x be a random variable whose possible values are between 0 and 1. The beta distribution is written [6]:

$$f(x) = \frac{1}{\beta(p,q)} x^{p-1} (1-x)^{q-1} \qquad (6)$$

With $p > 0$, $q > 0$ and:

$$\beta(p,q) = \int_0^1 x^{p-1} (1-x)^{q-1} \, dx = \frac{\Gamma(p)\,\Gamma(q)}{\Gamma(p+q)} \qquad (7)$$

With :

$$\Gamma(u) = \int_0^\infty x^{u-1} e^{-x} \, dx \qquad (8)$$

Where $u = p$, q or $p + q$

The possible values of the reflectivity factor are: $0 < Z \le Z_M$, where Z_M is the maximum value of this parameter. We can write: $0 < z = Z/Z_M \le 1$.

The probability that the reflectivity factor takes the Z value is then:

$$P(x \le z) = \int_0^z f(x)\,dx \qquad (9)$$

The mean and standard deviation of this distribution are:

$$\bar{x} = \frac{p}{p+q} \qquad (10)$$

We found the coefficients p and q equal to: $p = 106$, $q = 34$. To illustrate this model, we have represented in Fig.6, a calculated probability distribution (solid line) and obtained experimentally (dotted line). These curves show that the beta distributions smooth properly the frequency distribution of values of the reflectivity Z with coefficient of correlation equal to 0.95.

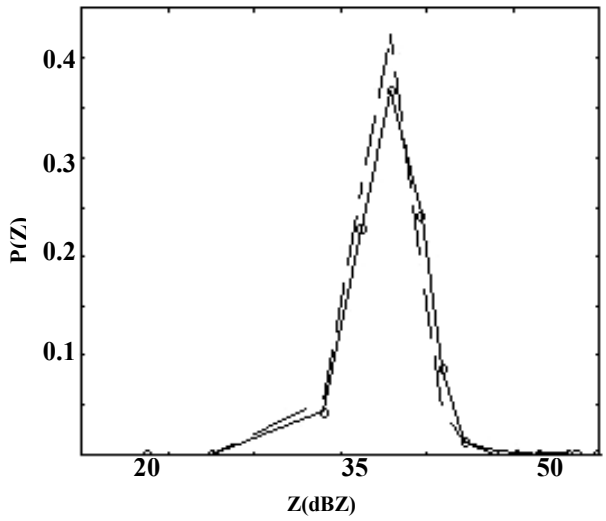

Fig. 6. Beta distribution associated with the log(z) for the study area ((o) experimental distribution (-) lognormal distribution).

5. Conclusions

Although the number of the reflectivity factor levels is limited to sixteen in radar images, we found that the

experimental distributions of the frequency of occurrence of these levels conform well as a log-normal distribution or a beta distribution. It seems to us that the Beta distribution gives better results for the modeling of atmospheric echo observed in the Sétif region. Note also that the reflectivity factor Z can also be modeled by another type of probability distribution for example the Rayleigh distribution [7]. In particular, we find that the most important atmospheric echo is observed in areas where rainfall is more intense. However, it should be mentioned that absence of any echo, Setif radar indicates a Z factor of between 8 and 16 dBZ when it should be close to zero. These results indicate that the radar must be calibrated to correct this scale shift.

The statistical properties of atmospheric cluster that we highlighted in this study could be usefully exploited in the methods of filtering the meteorological cluster echoes in the aviation observations.

6. References

[1] D. Renaut, Les satellites meteorologiques (Meteorological satellites), La Meteorologie. 2004,45 , 33-37.

[2] A. Meischner, Weather radar: principles and advanced applications. Springer, 2005.

[3] M.I. Skolnik,. Radar Handbook, Mc Graw Hill, New York, 2008.

[4] H. Sauvageot , Radar Meteorology. Artech House, Boston, 1992.

[5] O. Raaf, A. Adane: Pattern recognition filtering and bidimensional FFT-based detection of storms in meteorological radar images, Digital Signal Processing,, 2012, 22, 734-743.

[6] Spiegel, M.R. Série Schaum ; Probabilités et Statistiques, Mc Graw Hill, 1984, Paris

[7] Darricau, Y., Physique et théorie du radar, Tome I et II, , Ed. Sodye, 1993,Paris.